

28 **Introduction**

29 In modern high-speed railway lines *twin-box girder bridges* have become one of the
30 most popular solutions for spans between approximately 20 m and 45 m (Figure 1). This
31 success is attributable to their short construction time, which is largely due to the
32 prefabrication of the two main girders.



33

34 **Fig. 1.** Twin-box girder bridge on Madrid-Barcelona high-speed railway line. Characteristic
35 span length $L=30$ m

36

37 Significant dynamic effects may arise when transversely movable supports are
38 deployed in absence of diaphragms between the box girders. This configuration, which can be
39 found in high-speed lines such as the one connecting Spain and France or Madrid and
40 Barcelona (Burón and Peláez, 2002), induces potential resonance responses of the structure
41 that could seriously affect the upper concrete slab (excessive cracking, fatigue) if the dynamic
42 effects are not considered properly.

43 Some earlier studies on the subject do deal with transverse bending (Hamed and
44 Frostig 2005, Huang and Wang 1993, 1995, Rattigan et al. 2005), but very little has been said
45 about twin-box girder bridges. Cheung and Megnount (1991) conducted a study specifically

46 devoted to twin-box girder bridges. However it fails to consider the transverse distribution of
47 bending moments.

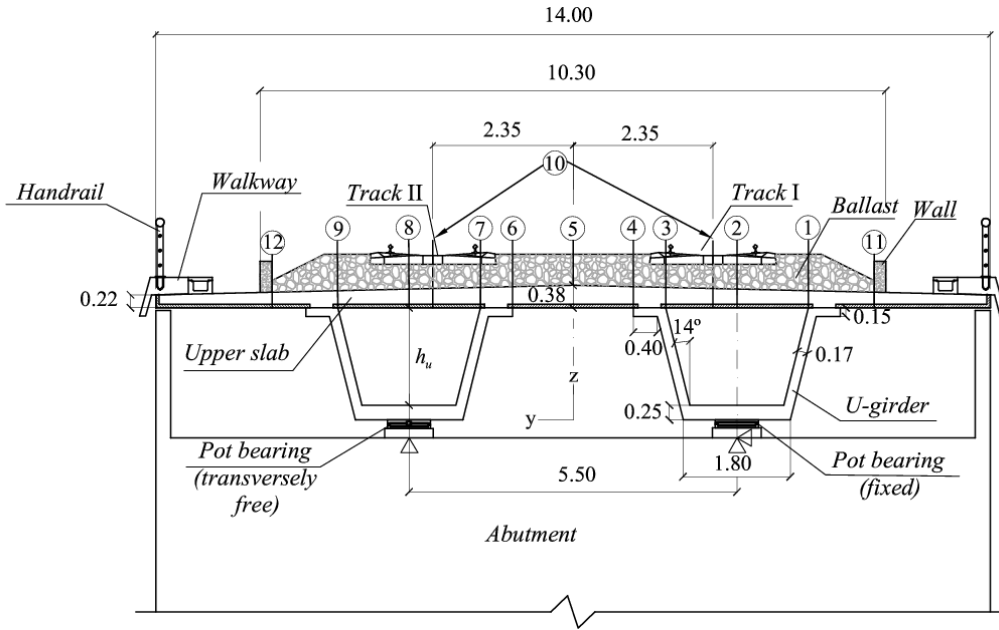
48 This work endeavors to launch a comprehensive study where several twin-box girder
49 bridges of increasing span length are analyzed. The numerical models used in this study
50 intentionally follow the prescriptions of Eurocode 1 (EC1) (CEN, EN 1991-2 2002), in an
51 attempt to show the predicted performance at the design stage. The influence of the
52 configuration of the supports on the dynamic response, particularly in the absence of
53 transverse diaphragms between the main girders, is one of the key issues with which this
54 paper is concerned.

55 **Twin-box girder bridges: case studies**

56 This study presents analysis results for four simply-supported decks of spans (20, 25,
57 30 and 35 m). Their main properties, shown in Figure 2 and Table 1, are derived from existing
58 structures so as to constitute realistic examples leading to meaningful results and conclusions.
59 The bridge deck consists of two prestressed, precast concrete U-shaped girders and a
60 reinforced concrete, cast in-situ upper slab. Each U-girder usually has rigid diaphragms at
61 both ends, where the hollow section is stiffened by a solid infill.

62

63



64

65 **Fig. 2.** Representative cross-section of a twin-box girder bridge and post-process points

66

L (m)		20	25	30	35
Upper slab	ρ (kg/m ³)	2500			
	f_{ck} (MPa)	35			
U-girders	h_u (m)	1.44	1.89	2.35	2.8
	ρ (kg/m ³)	2500			
	f_{ck} (MPa)	45			
	<i>Ballast+tracks</i> (kg/m)	11000			
Dead loads	<i>Walls</i> (kg/m)	480			
	<i>Walkways</i> (kg/m)	2450			
	<i>Handrails</i> (kg/m)	900			

67

Table 1. Main properties of the bridges

68

69

70

71

As regards the longitudinal constraints, both pots at one end are fixed and those at the opposite end are free. In a generic manner, the end of the deck where the longitudinal constraints are placed is referred to as *fixed abutment*.

72 **Numerical model**

73 *General aspects and assumptions*

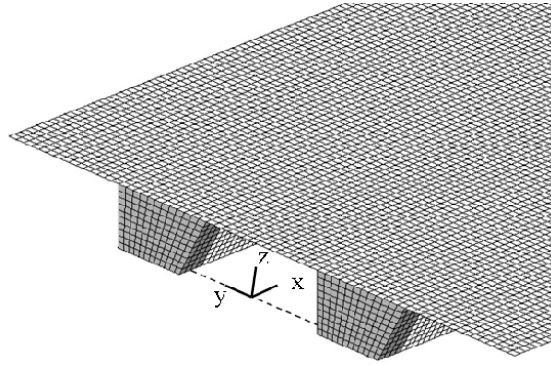
74 Two different linear elastic analyses were performed: static and transient dynamic
75 analysis solved by mode superposition under the action of railway traffic. With this purpose a
76 suitable finite element model (FEM) was devised. The meshing process, the static analyses
77 and the extraction of frequencies and mode shapes were performed using the commercial
78 code ANSYS, while the intensive computations associated with the passing of trains across
79 the bridges at different speeds were implemented with a suitable FORTRAN routine. This
80 routine carries out the time-integration by the Newmark- β linear acceleration algorithm, using
81 a time step equal to 1/25 times the smallest period among the modes considered.

82 A point load model is adopted for the railway excitation, following the European
83 standards. Therefore, train-bridge interaction is neglected in the analysis, which is also
84 supported by previous works (Doménech et al. 2014). The numerical model also disregards
85 track irregularities, since the regulations merely treat them by means of a multiplying factor.
86 The effects of soil-structure interaction are also neglected; this is usual in bridges supported
87 on short piles lying on a stiff foundation (Antolín et al. 2013; Liu et al. 2014).

88

89 *Deck geometry*

90 Figure 3 shows the mesh in the area near the abutments. The structure is discretized using
91 four-node shell elements with six degrees of freedom (dofs) per node and out-of-plane shear
92 deformation capabilities. For the rigid diaphragms at both ends of the girders (shaded
93 elements in Figure 3), eight-node hexahedral solid elements with three dofs per node were
94 used.



95

96

Fig. 3. FE mesh at the fixed abutment

97

All the elements have a length of 0.25 m in direction X. The size along direction Y (slabs) and direction Z (webs) does not remain constant for all the span lengths, but is rather similar. The average length in direction Y is 0.22 m for the upper slab and 0.14 m for the lower slab. Along the webs the average size is 0.18 m.

100

101

Permanent loads, e.g., ballast, track, walkways, etc., are distributed as additional masses of the elements of the upper slab. As regards the boundary conditions, the model considers pot bearings as ideal supports, a common assumption that previous research works also adopted (Majka and Hartnett 2009; Antolín et al. 2013). In the fixed abutment the bottom center node of the solid meshes at the diaphragm positions in each of the girders is constrained in the longitudinal and vertical directions (X and Z), whereas only one of them is fixed in transverse direction Y. At the opposite abutment the boundary conditions are identical except for the constraints in X, which are not present. Additionally, kinematic constraints are used in order to tie this restrained central node to a number of adjacent rows/columns of nodes, covering an area similar to the real pot dimensions.

102

103

104

105

106

107

108

109

110

111 ***Static and dynamic loads***

112

From a practical point of view it is customary to refer the maximum dynamic effects to some particular static load scenario by means of the so-called *impact coefficients*, i.e. the ratio between maximum dynamic and static values of the internal forces. As a common practice in

113

114

115 Europe, the reference static forces to be applied are the UIC-71 train defined in EC1, which
116 represents the static effect of vertical loading due to normal rail traffic. In this study the
117 variables of real interest are the dynamic internal forces; therefore the UIC-71 loads are
118 located in a convenient, straightforward position, acting symmetrically with respect to the
119 mid-span section.

120 The most unfavorable dynamic load usually occurs when the trains circulate at speeds
121 such that a given vibration mode experiences resonance. According to EC1 only one loaded
122 track is considered during the dynamic analyses, and the dynamic loads to be applied are the
123 10 trains prescribed in the High Speed Load Model A (HSLM-A model). They constitute an
124 envelope of the dynamic effects of the existing conventional high-speed trains.

125 **Description of the analyses and post-processing points**

126 The response of the four subject bridges is computed first in terms of transverse bending
127 moments under the static action of the UIC-71 loads placed at mid-span. These response
128 variables are then evaluated under the circulation of HSLM-A trains along each of the tracks
129 on the bridge (track I and track II, according to Figure 2) in two different ranges of velocities
130 of interest, which are [72, 420] km/h and [72, 540] km/h in steps of 3.6 km/h. The impact
131 coefficients are evaluated separately in each range of circulation speeds.

132 The static and dynamic results are computed at five sections {A, B, C, D, E}
133 corresponding to $x/L = \{0.25, 0.375, 0.5, 0.625, 0.75\}$, where L is the span length. In each
134 section several points for obtaining bending moments and also vertical accelerations are
135 considered. Figure 2 shows the locations of the points: transverse bending moments are
136 computed at points from 1 to 9, and accelerations are obtained at points 11, 10, 5 and 12.
137 Notice that when the loaded track is I, point 10 is located between points 2 and 3; conversely,
138 if the loaded track is II, point 10 is placed between 7 and 8.

139 **Results**

140 *Natural frequencies and mode shapes*

141 All the cases of study have a similar pattern in their mode shapes: the first three
142 eigenforms are global ones and they essentially govern the dynamic response; the modes
143 above the third one may be local or global, and their main effect on the internal forces is a
144 pseudo-static contribution. Table 2 gathers the natural frequencies of the first four eigenforms.

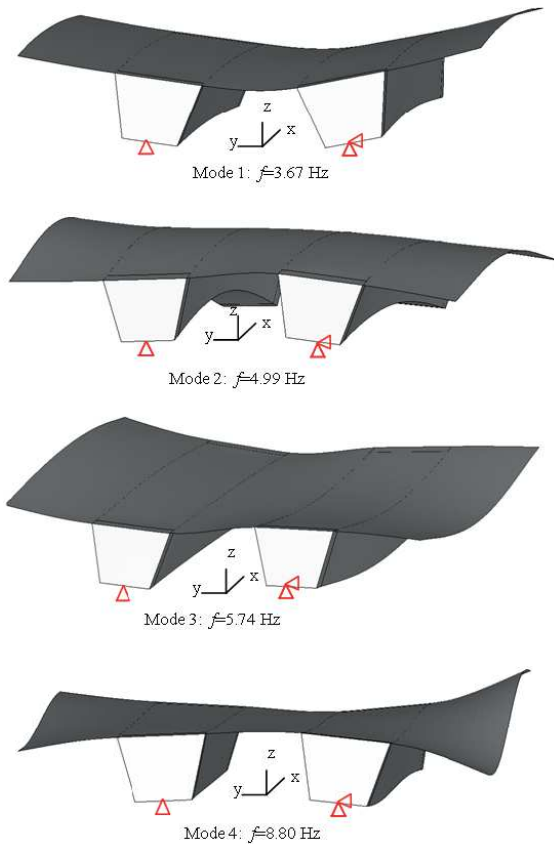
145

L (m)	1 st mode	2 nd mode	3 rd mode	4 th mode
20	4.141	5.750	6.230	9.288
25	3.671	4.991	5.741	8.803
30	3.232	4.335	5.512	8.191
35	2.862	3.822	5.329	7.428

146 **Table 2.** First four natural frequencies (Hz) of the bridges

147

148 Figure 4 shows the first four modes and their frequencies for the 25 m bridge. The first
149 mode is a transverse bending of the upper slab. In this eigenform the girders rotate as rigid
150 bodies and have little torsion, with also a limited longitudinal bending. In longitudinal
151 bending the U-girders do not behave as a single beam, but their main bending vibrations
152 correspond to modes 2 and 3 with similar frequencies and shapes: in both modes there is a
153 predominant longitudinal bending of one of the U-girders, complemented by a kind of rigid-
154 body rotation and a limited bending of the other. The bridges of span 20 m, 30 m and 35 m
155 feature similar mode shapes.



156

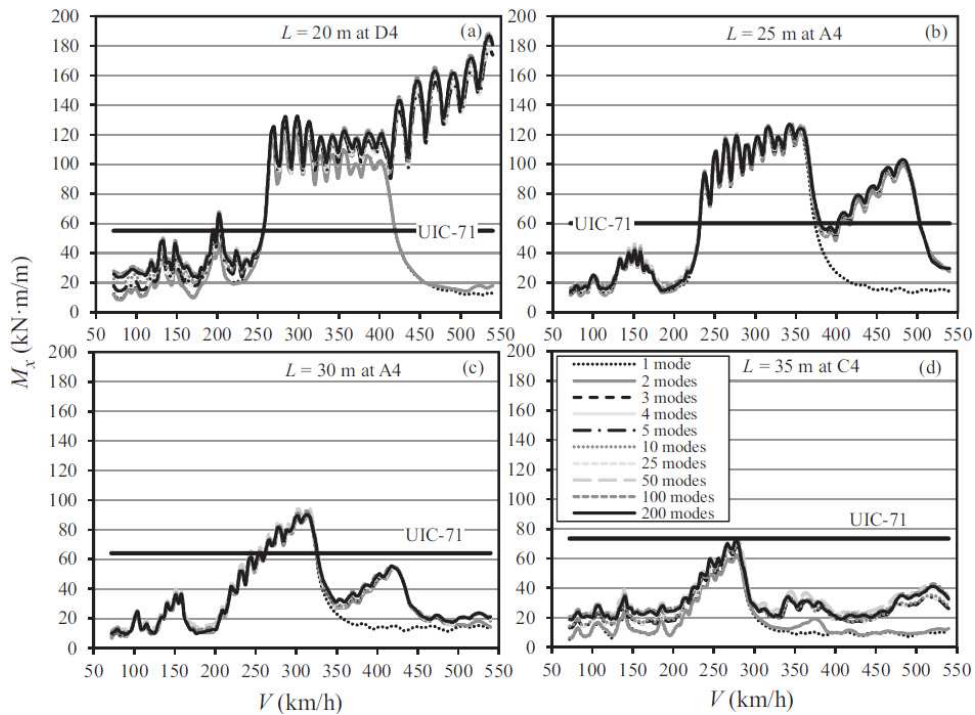
157

158

Fig. 4. First four vibration modes for the 25 m bridge

159 ***Envelopes of internal forces versus speed***

160 Figure 5 shows the maximum absolute values of transverse bending moment (M_x) due
 161 to the circulation of the HSLM-A trains at the most unfavorable post-process points. The
 162 values are plotted against the circulating speed for all bridges and for an increasing number of
 163 mode contributions (up to 200 modes, showing a satisfactory convergence). These results
 164 correspond to the circulation of the trains along track I, and a uniform damping ratio of 1% is
 165 assigned to all mode contributions following the prescriptions of EC1. For the sake of
 166 comparison, Figure 5 also shows the maximum absolute static value among all the post-
 167 process points under the action of the UIC-71 train. Particularly for the shortest structures, the
 168 maximum dynamic values largely exceed the static ones created by the UIC-71 design loads.



169

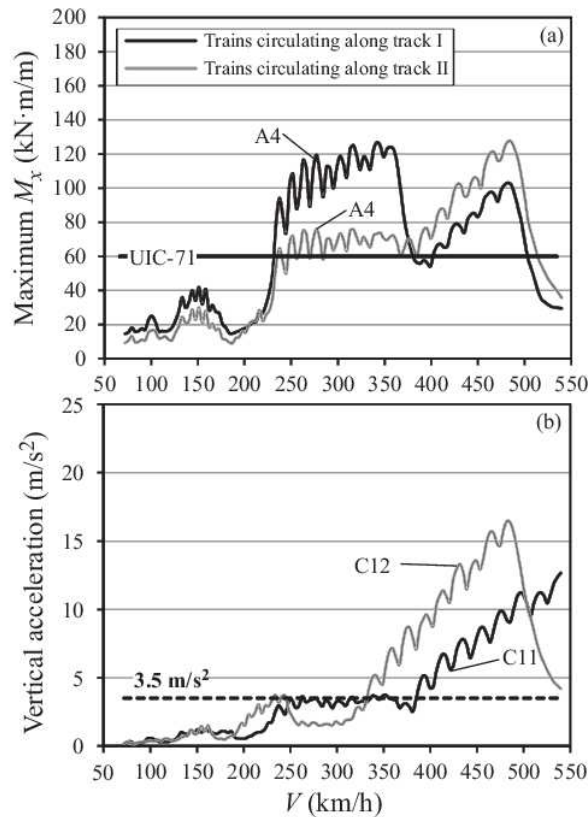
170 **Fig. 5.** Envelopes of maximum absolute transverse bending moments due to live loads. Trains
 171 circulating along track I. Legend in (d) applies to all subplots.

172

173 As can be seen in Figure 5, the maximum resonance peaks of the transverse bending
 174 moments are mainly governed by the contribution of the first eigenform at speeds below
 175 300–350 km/h, which is a frequent velocity limit in many high-speed railway lines. The
 176 contribution of the longitudinal bending modes is also noticeable at speeds higher than 350
 177 km/h, especially for the shortest spans ($L=20$ m, 25 m); but as the span length increases, the
 178 first mode prevails.

179 When the trains circulate along the opposite track (track II) the predominant mode
 180 contributions for each span length do not differ significantly from the results shown in Figure
 181 5. However, the influence of the loaded track on the dynamic response amplitude is in general
 182 quite noticeable. This is shown in Figure 6(a), where the transverse bending moment at the
 183 critical post-process points for the bridge of 25 m span is plotted, considering the contribution
 184 of the first 200 modes and the circulation of the trains alternatively along track I and track II,

185 in opposite directions. These results highlight that the dynamic behavior of twin-box girder
186 bridges under moving loads is clearly three-dimensional.



187
188 **Fig. 6.** Envelopes of maximum dynamic results for the 25 m bridge. (a) Transverse bending
189 moments; (b) vertical accelerations.

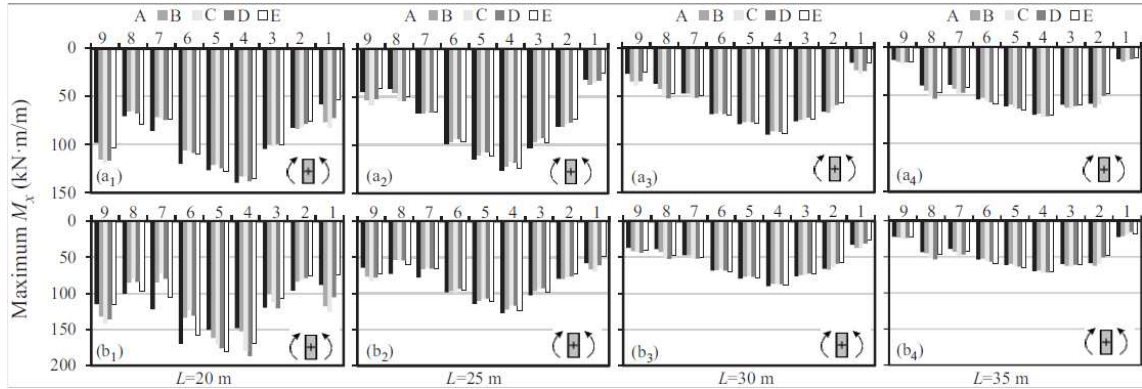
190

191 *Impact coefficients*

192 On a standard basis, the impact coefficients for transverse bending moments are used
193 for the design of the transverse reinforcement in the upper slab. In the initial design stages of
194 twin-box girder bridges, the coefficients presented in this section may thus provide a helpful
195 first estimate of what may be expected from transverse resonance phenomena.

196 The impact coefficient is evaluated as the quotient between the maximum dynamic
197 value in the upper slab and the maximum static one, both of them having the same sign. The
198 maximum static values used for the evaluation of the impact factors are obtained after placing

199 UIC-71 loads symmetrically along track II. The maximum dynamic transverse bending
 200 moments in the upper slab are positive, and are caused by the circulation of the trains along
 201 track I. They have been collected in Figure 7.



202
 203 **Fig. 7.** Envelopes of maximum positive transverse bending moments under the circulation of
 204 HSLM-A trains along tracks I and II. (a_i) $V_{max}=350 \times 1.2=420$ km/h; (b_i) $V_{max}=450 \times 1.2=540$
 205 km/h.

206 Table 3 gathers the impact coefficients for the bending moment considering maximum
 207 train speeds of 420 km/h and 540 km/h. It is seen that they are more affected by the increase
 208 in speed for the shortest span, while they remain almost constant when the velocity rises to
 209 540 km/h for the longest spans. Values higher than 2.0 are obtained in several cases. If not
 210 taken properly into account, this effect may have an influence on the transverse cracking of
 211 the concrete slab, which in turn may result in reductions in both the stiffness and the first
 212 natural frequency, thus leaving the bridge even more exposed to resonance phenomena (at
 213 lower speeds).

214

V_{max}	$L=20$ m	$L=25$ m	$L=30$ m	$L=35$ m
420 km/h	2.54	2.11	1.41	0.98
540 km/h	3.39	2.11	1.41	0.98

215 **Table 3.** Impact coefficients for transverse bending moment

216

217 ***Vertical accelerations***

218 The maximum level of vertical vibrations usually constitutes a critical Serviceability
219 Limit State (SLS) for other types of simply-supported high-speed bridges (ERRI D214/RP9
220 2001; Frýba 2001; EN 1991-2 2002; Museros and Alarcón 2005). The vertical accelerations
221 under the circulation of HSLM-A trains have been computed considering a maximum number
222 of mode contributions up to 30 Hz, which is a limit usually prescribed by structural codes
223 (ERRI D214/RP9 2001). The maximum peak values of the vertical acceleration of the bridge
224 deck calculated along each track shall not exceed 3.5 m/s^2 for ballasted tracks, according to
225 Eurocode (CEN, EN 1990-A2, 2005).

226 The analyses have shown that the 35 m bridge satisfies the 3.5 m/s^2 criterion in the
227 whole range of speeds. The 30 m bridge presents a good behavior up to 400 km/h
228 approximately. The 20 and 25 m bridges also behave well up to 350 km/h (approx.), where
229 resonances of the second and third modes start to increase the response significantly.
230 Consequently, the potential use of twin-box girder bridges for *very high-speed* lines ($V > 350$
231 km/h) should be examined with particular care.

232 Finally, Figure 6(b) shows the influence of the loaded track on the envelopes of
233 maximum acceleration versus speed, for the 25 m bridge. The most unfavorable circulating
234 track is not the same over the whole range of speeds, a fact that was also observed for
235 transverse bending moments, and underlines the importance of using three-dimensional
236 models in the dynamic analysis of this type of bridge.

237 **Conclusions**

238 In this work the dynamic response of several representative twin-box girder bridges under
239 high-speed railway traffic has been analyzed. The aim of this study was to investigate the
240 unusual performance predicted at the design stage when the transversally sliding bearings

241 beneath one of the U-girders are modelled as ideal rollers and without transverse diaphragms
242 between the box girders. The main conclusions are the following:

- 243 • The impact coefficients for transverse bending moments are higher than 2.0 and tend
244 to decrease with the span length. Such extreme values highlight the need for future
245 research work to support or contradict whether they are excessively conservative due
246 to other effects that should be considered in the calculations, such as a performance of
247 the pot bearings far from the ideal behavior implemented in most numerical models.
- 248 • At speeds below 350 km/h the transverse bending moments are mainly governed by
249 resonances of the first eigenform. The introduction of diaphragms or cross-bracings
250 between the girders could significantly reduce those transverse bending moments in
251 spite of a certain amount of complexity being added to the construction process. This
252 stiffening measure would be in line with the California codal recommendation of the
253 first torsional frequency being at least 1.2 times greater than the first vertical bending
254 frequency. Such interpretation of this code would be reasonable from an engineering
255 point of view, given that the first eigenform is not a torsional mode but a transverse
256 bending one that is not contemplated in (California High-Speed rail Authority 2014).
- 257 • The potential use of twin-box girder bridges for very high-speed lines ($V > 350$ km/h
258 approx.) should be examined with particular care due to excessively high vertical
259 accelerations appearing in the ballast. Structures that are stiffer and more massive than
260 the ones analyzed in this paper could be required to satisfy the acceleration SLS
261 (3.5 m/s^2) at such very fast speeds.
- 262 • The dynamic behavior of twin-box girder bridges under moving loads is clearly three-
263 dimensional: the contribution of the first transverse bending mode to the
264 corresponding bending moments and the influence of the loaded track are significant.

265 **Acknowledgements**

266 This research was supported by the State Secretariat for Research of the Spanish Ministry of
267 Science and Innovation (Secretaría de Estado de Investigación, Ministerio de Ciencia e
268 Innovación, MICINN) in the framework of Research Project BIA2008-04111. The authors
269 also gratefully acknowledge the collaboration of Mr. A. Castillo-Linares in this investigation.

270 **References**

- 271 Antolín, P, Zhang, N, Goicolea, J.M., Xia, H, Astiz, M.A. and Oliva J. (2013). “Consideration
272 of nonlinear wheel–rail contact forces for dynamic vehicle–bridge interaction in high-speed
273 railways”. *J Sound Vib*, 332, 1231-1251.
- 274 Burón M., Peláez. (2002). “Puentes para el ferrocarril de alta velocidad con tablero
275 prefabricado”. II Congreso de ACHE de Puentes y Estructuras, Madrid.
- 276 CEN (2002). EN 1991-2. *Eurocode 1: Actions on Structures - Part 2: Traffic loads on*
277 *bridges*. Brussels: European Committee for Standardization.
- 278 CEN (2005). EN 1990-A2. *Eurocode: Basis of structural design*. Annex A2, application for
279 bridges. Final version. Brussels: European Committee for Standardization.
- 280 California High-Speed rail Authority (2014). Request for proposals for Design-Build Services
281 for Construction Package 2-3. Book III, Part A, Design criteria manual. Rapport n°: HSR 13-
282 57.
- 283 Cheung, M.S., and Megnounit, A. (1991). “Parametric study of design variations on the
284 vibration modes of box girder bridges”. *Canadian Journal of Civil Engineering*, 18, 789-798.
- 285 Doménech, A., Museros, P., Martínez-Rodrigo, M.D. (2014). “Influence of the vehicle model
286 on the prediction of the maximum bending response of simply-supported bridges under high-
287 speed railway traffic”. *Engineering Structures*, 72, 123-139.
- 288 ERRI D214/RP9 (2001). *Railway bridges for speeds >200 km/h. (Final Report)* Utrecht:
289 European Rail Research Institute (ERRI).
- 290 Frýba L. (2001) “A rough assessment of railway bridges for high speed trains”. *Eng Struct*,
291 23, 548–556.
- 292 Hamed, E., and Frostig, Y. (2005). “Free vibrations of multi-girder and multi-cell box bridges
293 with transverse deformations effects”. *J Sound Vib*, 279, 699-722.

294 Huang, D., Wang, T.L., and Shahawy, M. (1993). "Impact studies of multigirder concrete
295 bridges". *Journal of Structural Engineering, ASCE*, 119, 2387-2402.

296 Huang, D., Wang, T.L., and Shahawy, M. (1995). "Vibration of thin-walled box-girder
297 bridges excited by vehicles". *Journal of Structural Engineering, ASCE*, 121, 1330-1337.

298 Liu K, Lombaert G, and De Roeck G. (2014). "Dynamic analysis of multispan viaducts with
299 weak coupling between adjacent spans". *Journal of Bridge Engineering*, 19, 83-90.

300 Majka, M., and Hartnett, M. (2009). "Dynamic response of bridges to moving trains: A study
301 on effects of random track irregularities and bridge skewness". *Computers & Structures*, 87,
302 1233-1252.

303 Rattigan, P.H., González, A., O'Brien, E.J., and Brady S.P. (2005). "Transverse variation of
304 dynamic effects on beam-and-slab medium span bridges". In *Proceedings of the sixth*
305 *European conference on structural dynamics*, 1643-1648.

306